Available online at www.sciencedirect.com

ScienceDirect

Procedia Manufacturing 26 (2018) 1014–1022

Procedia MANUFACTURING

www.elsevier.com/locate/procedia

46th SME North American Manufacturing Research Conference, NAMRC 46, Texas, USA

Investigation of Layer Based Thermal Behavior in Fused Deposition Modeling Process by Infrared Thermography

Ehsan Malekipour[a,*], Samuel Attoye[b], Hazim El-Mounayri[c]

[a,b,c] *Collaborative Additive Manufacturing Research Initiative at IUPUI (CAMRI)*
Purdue School of Engineering and Technology, Indianapolis, IN, 46202, USA

* Corresponding author. Tel: +1-317-993-6659
E-mail address: emalekip@purdue.edu

Abstract

There are numerous research efforts that address the monitoring and control of additive manufacturing (AM) processes to improve part quality. Much less research exists on process monitoring and control of Fused Deposition Modeling (FDM). FDM is inherently a thermal process and thus, lends itself to being study by thermography. In this regard, there are various process parameters or process signatures such as built-bed temperature, temperature mapping of parts during deposition of layers, and the nozzle extrusion temperature that may monitor to optimize the quality of fabricated parts. In this work, we applied image based thermography layer by layer with the usage of an infrared camera to investigate the thermal behavior and thermal evolution of the FDM process for the standard samples printed by ABS filament. The combination of the layer based temperature profile plot and the temporal plot has been utilized to understand the temperature distribution and average temperature through the layers under fabrication. This information provides insights for potential modification of the scan strategy and optimization of process parameters in future research, based on the thermal evolution. Accordingly, this can reduce some frequent defects which have roots in thermal characteristics of the deposited layers and also, improve the surface quality and/or mechanical properties of the fabricated parts. In addition, this approach for monitoring the process will allow manufacturers to build, qualify, and certify parts with greater throughput and accelerate the proliferation of products into high-quality applications.

Peer-review under responsibility of the scientific committee of the 46th SME North American Manufacturing Research Conference.

Keywords: additive manufacturing; fuesd deposition modeling; online monitoring; infrared thermography; thermal evolution; thermal behavior

1. Introduction

Fused deposition modeling (FDM) is inherently a thermal process and thus, the quality of the final part depends significantly on the thermal evolution of the process. For instance, one critical thermal step in the FDM process is increasing the temperature of the material (polymer) up to its glass transition temperature. This temperature refers to the state at

2351-9789
Peer-review under responsibility of the scientific committee of the 46th SME North American Manufacturing Research Conference.
10.1016/j.promfg.2018.07.133

which amorphous phase commences and it is different from melting temperature [1]. Studies by Sun et al in 2008 and Berretta et al in 2017 suggest that at these levels, the polymer viscosity reduces and its flow increases [2, 3]. In this respect, controlling of the nozzle temperature significance as a process parameter [4]. Another thermal fact is an instant hardening of the deposited material as it fuses to the layer beneath [1]. As soon as the layer is fabricated, another layer is deposited by the extrusion nozzle. The FDM process is not a flawless process. The materials characteristics, the difficulties in printing finely-detailed items (3D printer limitations), discerning of optimized process parameters, and unfavorable/uncontrolled thermal aspects of the process, are the essential contributing items lead to some process defects. While current AM machine tools are greatly improved from early versions, many of the same problems identified by early researchers in the 1980s persist [5]. Some of these defects directly have root in thermal characteristics and also, the temperature distribution of deposited layers. Warping and curling, for instances, are significantly dependent on the thermal interaction between the current layer and the layers fabricated earlier. As Fig. 1 shows, these defects refer to the printed part curving or bending upwards from the platform. The top layer contracts relative to the bottom layer since the new layer possess a higher temperature than preceding one. The warping is created by the thermal stresses caused by the temperature gradient between the layers [5-7]. These aspects of FDM process, suggest monitoring of the temperature distribution and thermal evolution of parts during deposition of layers, as a key towards a better understanding of the process. This information can also utilize in the future to control of the process parameters for favorable temperature evaluation and thus, reaching a better quality. In addition, monitoring and control will allow industries to build, qualify, and certify parts for higher performance application [8, 9]. performance application [8, 9]. Currently, many machine condition monitoring strategies are based on two types of models, physics-based models and data-driven (empirical) models. The first type of models predicts the phenomena of systems with the consideration of physical natures and mechanisms of the systems whereas, the second type utilizes historical data only to build analytical models for product property or failure predictions [10]. According to the study by Everton et al. in 2015, the lack of an inbuilt system to study the on-going fabrication process of 3D

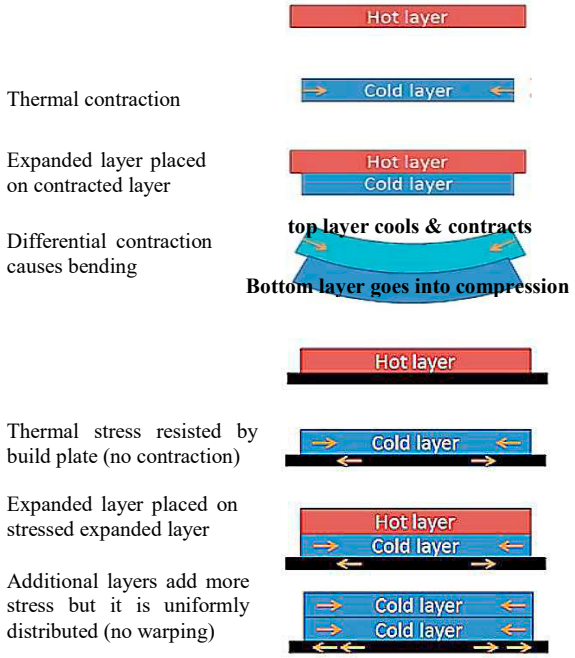

Figure 1: Cooling of build layers and part contraction in FDM process

printer, and closed-loop control algorithms makes manufacturers adjust process parameters. This adjustment is based on heuristics from previous fabrication runs, yielding limited improvement in part quality, and requiring many builds run for convergence [9, 11]. Basically, a typical machine condition monitoring sequence includes sensing and data collection, data processing and feature extraction, cognitive decision making, and action (selection of optimized process variable) [10, 12]. In this regard, there has always been a constant effort for employing of different methods and process measurement to monitor AM processes; however, much less research exists on process monitoring and control of FDM to improve quality parts. In one recent effort, Cummings et al in 2016 used ultrasonic excitation as a mean of detecting filament bonding failures introduced by manipulating the print bed temperature during the fused deposition modeling build process [13]. In another effort, Wu et al. in 2016 proposed a new method for in-situ monitoring of FDM machine conditions through the application of acoustic emission (AE) technique [10]. The proposed method allowed for the identification of both normal and abnormal states of the machine conditions. Furthermore, as Krauss H., et al reported in 2012, infrared thermography has been employed in quite a number of study concerning process monitoring in additive manufacturing. Most of these studies are

based on selective laser melting (SLM) since it is a thermal process [14]. Thermography can also be suitably used to monitor the FDM process because it is inherently a thermal process. Studies by Kousiatza et al in 2017 show enumerated temperatures within the chamber, temperature mapping of parts during deposition of layers, and the nozzle extrusion temperature as the parameters for monitoring and control in the FDM process [15]. Zhou Z., et al in 2017 also developed an experimental model to aid in applying a cost-effective infrared thermography imaging method, to acquire temperature history of filaments at the interface and their corresponding cooling mechanism to map the temperature within the build volume of the oven [16]. The use of thermography for process monitoring in FDM was very promising, however, the literature on it is very limited. In this regard, we perform a real-time monitoring of FDM process of ABS plastic to investigate the thermal evolution and thermal behaviour such as quantify the temperature distribution through the printing layers, the average temperature of printing layers, comparing the thermal evolution/behavior of the specimens printed in different orientations, etc. during part evolution. Interpretation of these thermal data can be assisted to potential offline/online modification of the scan strategy in future research for each and every layer.

2. Methodology and experimental setup:

The specimen selected for monitoring and evaluation is based on the ASTM tensile strength test standard part. The dimensions of the sample with minor adjustments to facilitate the printing process are shown in Fig. 2. Twenty-seven different specimens were printed and monitored to understand the thermal evolution through the fabrication of parts while the printing process parameters, namely, nozzle temperature, printing speed, and print orientation were adjusted for each part. An Air-Wolf FDM 3-D printer was used to fabricate the specimens. The 30% infill density, honeycomb fill pattern, and rectilinear top/bottom layers fill pattern are utilized to print the specimens. The printing parameter values were selected based on the machine and material specifications. The material used for printing the specimens was Filabot ABS 1.75 mm. The build orientation, shown in Fig. 3, was adjusted in the X, Y and Z orientations. A FLIR IR camera A325 series (Fig. 4.a) interfaced with the Research IR Max software student test version (Fig. 4.b) was used for monitoring the process and acquiring the thermal data. The fabrication process was monitored and the results were analyzed and revealed in section 3.

Table 1: printing parameters adjusted for fabrication process of specimen S1-S27

Printing parameters	Parameters values		
Nozzle temperature in °C	215	225	235
Printing speed in mm/s	20	40	60

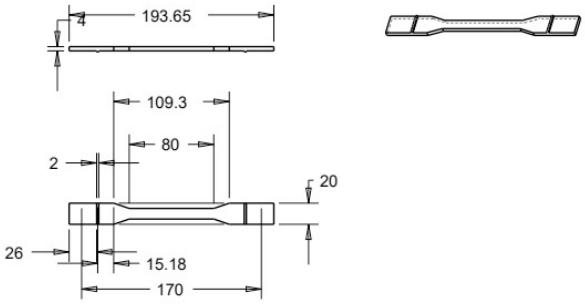

Figure 2: The modified ASTM tensile strength sample used for printing

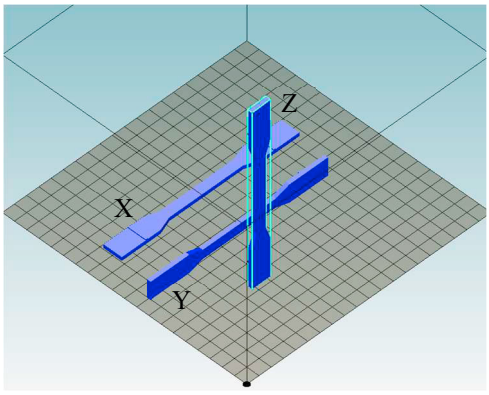

Figure 3: X, Y, and Z build orientation used in fabrication of the specimens

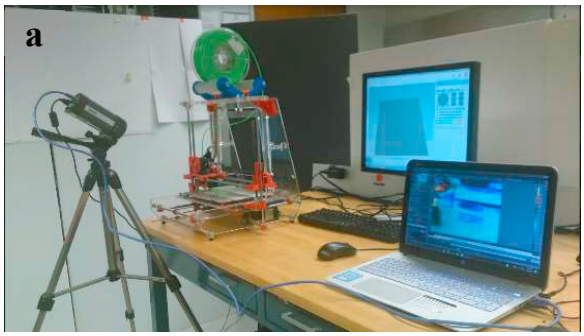

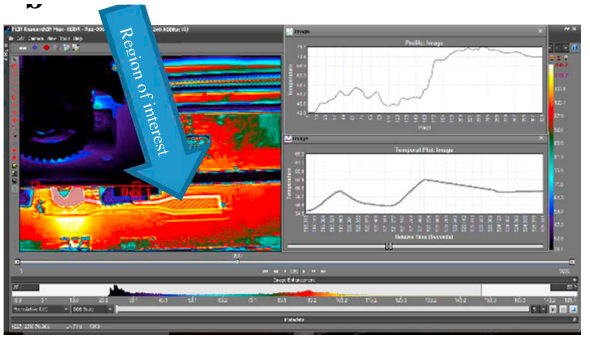

Figure 4: a. Monitoring the FDM process on the Air-Wolf 3D printer with FLIR IR camera A325; b. The Research IR Max software GUI to measure thermal evolution of the fabrication process

3. Results and discussion

3.1. Thermography Results from the specimens fabricated on the AirWolf 3-D printer

The Research IR Max software graphical user interface (GUI) is utilized for the in-situ monitoring of fabrication process (Fig. 4.b). The infrared real-time video shows the deposited material during fabrication of the part in successive layers on the GUI left. The temperature profile on the GUI top right (see Fig. 5.a as an example) shows the average temperature in the column of pixels in the monitored region of interest (ROI) (see Fig. 4). Thus, providing information on the average temperature and temperature distribution over the built layer surface. In this case, the ROI is the region showing layer-wise material deposition process as the specimen individual layers are being built. The temporal plot, placed on the GUI bottom right (see Fig. 5.b as an example), provides information on the part build temperature distribution across the layer surface with respect to printing time.

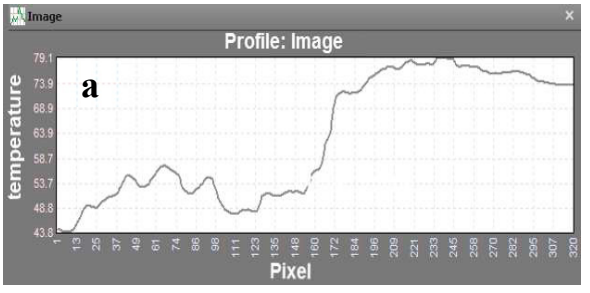

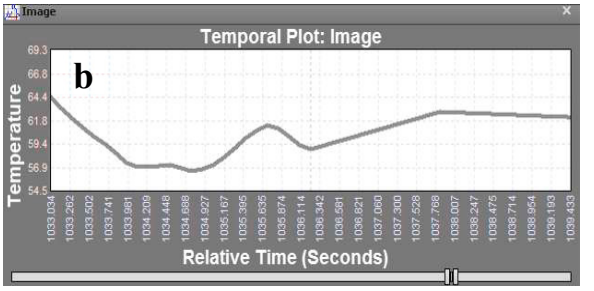

Figure 5:a. An example of temperature profile; b. an example of temporal plot

3.2. Temperature profile plot trends

Three generic plot trends (Fig. 6) were observed during the monitoring process of the specimens in the X, Y, and Z -axis orientation. These plots were observed to occur based on the starting point of the printer nozzle, the printed direction of the previous layer, and the pattern followed in the material deposition.

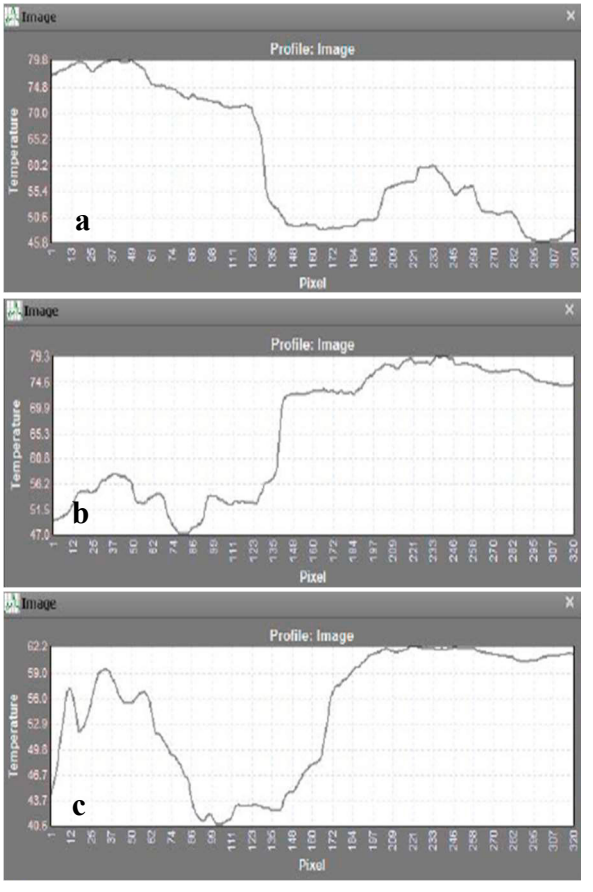

Figure 6: a, b, and c; Generic plot trends observed during monitoring process of printing the specimen

In the temperature profile plot trend shown in Fig. 6.a, average temperature retrieved from the ROI column of pixels is initially high; then gradually reduces in magnitude. This occurs when the material deposition pattern begins from the geometric origin of the layer being printed then follows along the entire length of the specimen to the geometric endpoint of layer being printed. In the temperature profile plot trend shown in Fig. 6.b, average temperature retrieved from the ROI column of pixels is initially low; then gradually increases in magnitude. This occurs when the material deposition pattern begins from the geometric endpoint of the layer being printed then follows along the entire length of the specimen to the geometric origin of the layer being printed. In the temperature profile plot trend shown in Fig. 6.c, average temperature retrieved from the ROI column of pixels is initially high and although gradually reduces in magnitude; begins again to gradually increases in magnitude. This occurs in two statuses. The first status is when the material deposition pattern begins either from the geometric origin or endpoint of layer being printed. Then continues to a point along the length of the specimen layer being printed. It then skips to the opposite end of that layer and begins to deposit material while returning to the skip-point. We also observe this trend in the temperature profile plot while the first or last number of layers are printed for the specimen in Y-orientation. As Fig. 3 shows, in these layers the printing cross-sectional areas exist just in the left and right hand side of the layers and thus, the temperature of the middle of the layers falls down. These material deposition patterns (print strategy) were repeated as the successive layers were built.

3.3. Temporal plot interpretation

As it was already mentioned, the temporal plot provides information on the layer surface temperature distribution through the specimen built layers with respect to time elapsed. The nature of the generated curves can be interpreted to determine the part layer-wise thermal evolution and the uniformity of heat in successive part built layers. The layer surface temperature is influenced by the interaction between the heat affected zone (HAZ), the area closest to the printer nozzle as the material being deposited, and the already deposited material. In observing the temporal plot, a smooth plot suggests a more evenly distributed temperature at the layer being built and preceding layers. These smoother plots were observed to occur more during printing of last layers in the y-axis orientation and x-axis orientation. While the temporal plots of the initial layers of the specimens were seen to have more fluctuations, than the specimen mid and final build layers. For an instance, the temporal plot for the layer 6 and layer 30 of specimen S4 compared together in Fig. 7. The source of these fluctuations in the plot is the temperature differences between the interacting regions, namely, HAZ, the already deposited material on that layer, and also previously built layers. Considering these explanation, it should be clear the reasons why the temporal plots of the initial layers of the specimens were seen to have more fluctuations than the specimen mid and final build layers. Practically, the availability of more deposited material in the mid and final build layers that serve as heat sink facilitate more even distribution of temperature with respect to time at the layer and between the already built layers. In Fig. 7, for an instance, we can see that the temporal plot in initial layers indicates significant fluctuation and the temperature differences between the interacting regions is about 10 °C. By passing more time, although the temporal plot shows initial irregularity, it gradually begins to show more evenness. At layer 30, the fabrication is almost complete and the temperature differences decline to about 3.8 °C.

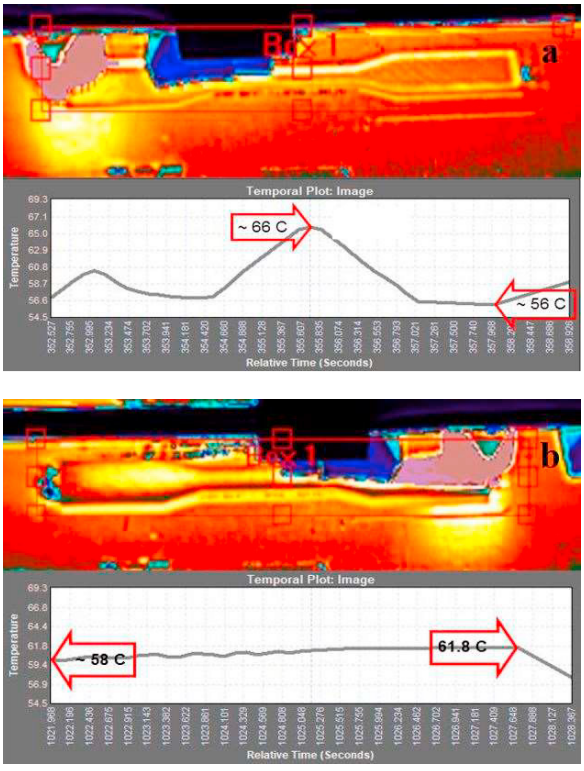

Figure 7: a. Thermal evolution and plot for specimen S4 layer 6; b. Thermal evolution and plot for specimen S4 layer 30

It is noteworthy that changing the cross-sectional area may also affect the plot. Larger printed area leads to higher average temperature. However, for the specimens printed here in Y and Z directions, the effect of changing the cross-sectional area versus the thermal effect of the already deposited material of previous layers were negligible. Another source of these fluctuations in the temporal plots during printing of the part are attributed to the presence of intermittent pores and dense regions in the specimen being built (Fig. 8.a). This source of fluctuation in temporal plot can be seen especially for the specimens printed in X and Y-axis orientation. It was, however, observed that the temporal plots are predominantly uniform for the Z-axis orientation (Fig.8.b). This happens because of small cross-section, short printing time for each layer, and thus, less temperature gradient between different zones of each layer.

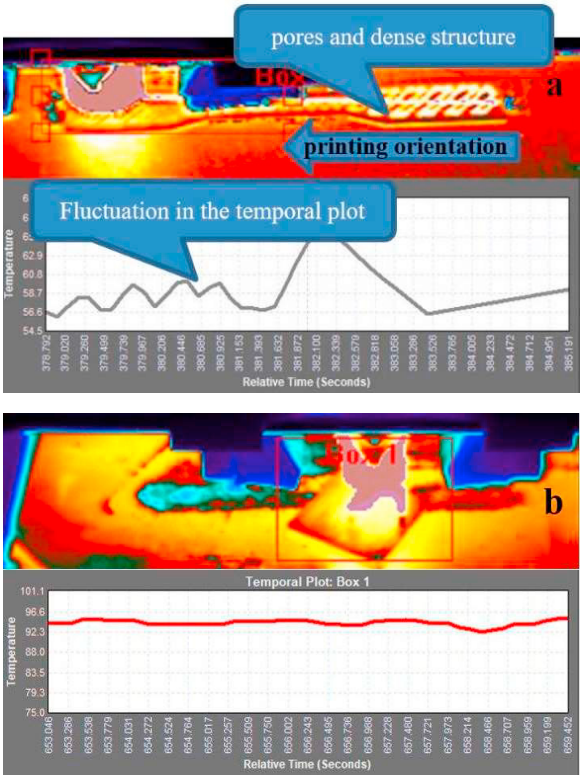

Figure 8: a. a layer with pores and dense and its fluctuating temporal plot; b. a specimen printed in Z-axis and its uniform temporal plot

3.4. Comparison of thermal evolution between different printing orientation

The combination of the layer-wise temperature profile plot and temporal plot provide insights for specimens fabricated in different orientations. The specimens printed in the X-axis orientation required 35 layers to be built. As it was explained in the previous section, the thermal trend in this orientation suggests a low uniformity in temperature changes between the earlier layers (see Fig. 7.a as an example). The temperature profile shows that in layer 1 the temperature for the specimens with different process parameters distributed across the surface with the range of 42.7 ℃ to 79.1℃. The average of this range (T_{ave} is 60.9 °C) shows the average temperature of the first layer. We can see that this value is very close to the average temperature of the whole process until that moment, that is obtained from the temporal plot. The temporal plot has a range between 54.5℃ to 65.1℃ whose average is 59.8 °C. At the mid layer (layer 17) the temperature, shown in temperature profile plot, distributed across the surface with the range of 44.5 ℃ to 78.7℃ with the average of 61.6 °C and in the temporal plot has a range between 60.8℃ to 62.9℃ with the average of 61.8 ℃ which is again very close to the average temperature derived from the temperature profile plot. We also can see that the average temperature of the whole process is increased 2 °C until this moment (it reaches from 59.8 °C to 61.8 °C) . Finally, at the final layer (layer 35), the temperature profile shows the temperature, distributed across the surface, with the range of 45.4 ℃ to 78.8℃ with the average of 62.1 °C. The temporal plot has a range between 64.4℃ to 66.8℃ with the average of 65.6 °C which shows 5.8 °C increase in the average temperature of the whole process since the first layer fabricated. The specimens printed in the Y-axis orientation required 59 layers and the ones printed in the Z-axis orientation required 1256 layers to be built. A similar thermal evolution was observed for these orientations. In Y-axis orientation, the average temperature of the whole process increased 4.4 °C (from 54.9 °C in the first layer to 59.3 °C in layer 59) and in Z-axis orientation, the average temperature of the whole process increased 8 °C (from 48.2 °C in the first layer to 56.2 °C in layer 1256). The increase in the average temperature from beginning to the end of process mentions that the parts printed in Z, X, and Y-axis orientation have respectively the highest amount of heat accumulation. Our observations show that there are four factors affect the heat accumulation during the fabrication of specimens. First and foremost, the time elapsed between the deposition of layers. The shorter the time is, the less time remains for heat dissipation and thus, the average temperature will increase more. Second, the size of the cross-section. The bigger size of cross-section leads to absorbing heat more and thus, increase the heat

accumulation. Third, the nozzle temperature. Increasing the nozzle temperature raise up the filament temperature that injects from the nozzle. This affects the average temperature of the deposited material. The final reason is the number of layers. More layers to deposit, more temperature increases. As Fig. 3 shows, according to these factors however the part printed in Z-axis orientation has the smallest cross-section compared with the specimens printed in the other two orientations, it leads to a very short time between layer deposition and thus, more heat accumulation. Also, the number of layers in this orientation is significantly higher than the specimens printed in the other two orientations. On the other hand, the number of the layers for the specimens printed in X and Y direction is close to each other but the part printed in X orientation has a bigger cross-section and thus, absorb more heat during the process.

3.5. Monitoring of thermal behavior to enhance mechanical properties

In this stage, we perform the tensile test on twenty-seven printed specimens whose thermal data already monitored during the fabrication process. Table 1 shows the process parameters used for printing the specimens. In these experiments, there are some uncertainty parameters affect the thermal evolution of the part under fabrication such as the ambient condition, the printer precision, etc. In most cases, the information derived from observing the temperature profile and temporal plot, suggest that a fabrication process with more even temperature distribution across individual build layers and through the part layers would facilitate better mechanical properties. However, the process parameters have a significant effect on the final mechanical properties of fabricated parts. Fig. 9 shows the maximum mechanical properties, obtained from performing of the tensile test for different process parameters [4]. The role of thermal evolution cannot be ignored. The monitoring of temperature distribution, the average temperature gradient between the fabricated layers can be utilized for modification of scan strategies, the pause between layer fabrication to make enough time for adequate heat dissipation, and also printers chamber conditions in order to reach more uniform temperature distribution during fabrication. Furthermore, examining of the specimens printed in Z-axis orientation shows the necessity of controlling the average temperature, obtained from the temporal plot, to compromise between good mechanical properties and final surface condition. In this orientation, increasing the average temperature of the fabricated layers, either by increasing the nozzle temperature or reducing the printing speed, improved some mechanical properties but reduced the surface condition. Thus, the average temperature may be utilized as a criteria for obtaining the optimized set of nozzle temperature and printing speed in order to achieve the desired mechanical properties and surface condition. This can happen by controlling of process parameters such as printing speed, pausing between layer fabrication, nozzle temperature, and airflow speed in the printer chamber.

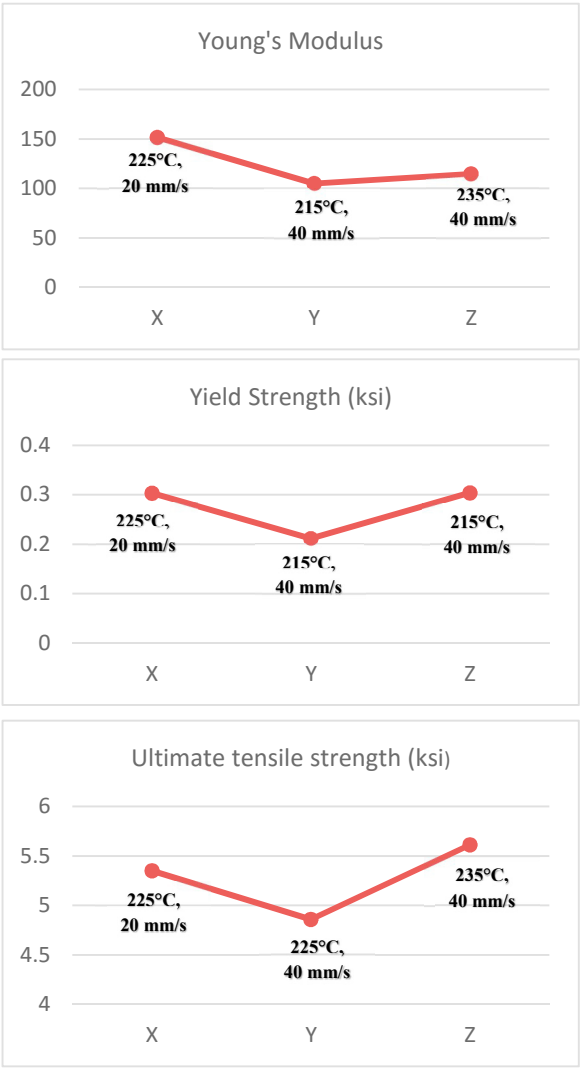

Figure 9: The maximum mechanical properties of the printed specimens

4. Conclusions and future works

This research work presents thermal experiments analysis and parameters effects on FDM process. The study also employs an in-situ monitoring technique to track the thermal evolution in the fabrication process. The combination of the layer-wise temperature profile plot and temporal plot provide insights for specimens fabricated in X, Y, and Z-axis orientation. The thermal trend through the evolution of the specimen seen in the thermal profile plot suggests a low uniformity in temperature changes between the earlier layers and more even distribution as the build progresses through the half to the final layers. The thermal measurement also showed the influence of the temporal average temperature of the part under fabrication on its final quality. The information retrieved from observing the temperature profile and temporal plot, suggest that a fabrication process with more even temperature distribution across individual build layers and through the part layers would facilitate better mechanical properties. It was observed that the ambient temperature, infill scan pattern, and infill density also would have significant effects on the thermal evolution of the build layers. In this work all the experiments carried out in a standard room temperature condition, with the same mentioned scan strategy. The effects of altering the ambient temperature and scan strategy were not investigated. More precise results with same profiles' trends are predicted to be acquired for the experiments printed in a sealed chamber. These could be controlled and studied in future research. Correlating of printing parameters and thermal evolution with the microstructural characteristics of the specimens would also provide more insights in this subject matter. In addition to the aforementioned points, the image monitoring, processing techniques and results analysis derived from this work can be applied in real-time monitoring and control of metal additive manufacturing technologies.

References

[1] M. Chanda and S. K. Roy, *Plastics technology handbook*: CRC press, 2006.

[2] Q. Sun, G. Rizvi, C. Bellehumeur, and P. Gu, "Effect of processing conditions on the bonding quality of FDM polymer filaments," *Rapid Prototyping Journal,* vol. 14, pp. 72-80, 2008.

[3] S. Berretta, R. Davies, Y. Shyng, Y. Wang, and O. Ghita, "Fused Deposition Modelling of high temperature polymers: Exploring CNT PEEK composites," *Polymer Testing,* vol. 63, pp. 251-262, 2017.

[4] S. Attoye, E. Malekipour, and H. El-Mounayri, "Correlation between process parameters and mechanical properties in parts printed by FDM process," *Under preparation,* 2018.

[5] N. K. Spinnie, "Large scale fused deposition modeling: the effect of process parameters on bead geometry," 2016.

[6] J. Li, *Engineering Plasticity and Its Applications: Proceedings of the 10th Asia-Pacific Conference, Wuhan, China, 15-17 November 2010*: World Scientific, 2011.

[7] R. Orlando, V. Kunc, C. Duty, and L. Love, "Electromagnetic blunting of defects within fused deposition modeling (fdm) components," ed: Google Patents, 2015.

[8] S. Clijsters, T. Craeghs, S. Buls, K. Kempen, and J.-P. Kruth, "In situ quality control of the selective laser melting process using a high-speed, real-time melt pool monitoring system," *The International Journal of Advanced Manufacturing Technology,* vol. 75, pp. 1089-1101, 2014.

[9] S. K. Everton, M. Hirsch, P. Stravroulakis, R. K. Leach, and A. T. Clare, "Review of in-situ process monitoring and in-situ metrology for metal additive manufacturing," *Materials & Design,* vol. 95, pp. 431-445, 2016.

[10] H. Wu, Y. Wang, and Z. Yu, "In situ monitoring of FDM machine condition via acoustic emission," *The International Journal of Advanced Manufacturing Technology,* vol. 84, pp. 1483-1495, 2016.

[11] D. L. Russell, "Real-Time Monitoring and Control of Additive Manufacturing Processes," 2014.

[12] M. Elbestawi and M. Dumitrescu, "Tool condition monitoring in machining-neural networks," *Information Technology for Balanced Manufacturing Systems,* pp. 5-16, 2006.

[13] I. Cummings, E. Hillstrom, R. Newton, E. Flynn, and A. Wachtor, "In-process ultrasonic inspection of additive manufactured parts," in *Topics in Modal Analysis & Testing, Volume 10*, ed: Springer, 2016, pp. 235-247.

[14] H. Krauss, C. Eschey, and M. Zaeh, "Thermography for monitoring the selective laser melting process," in *Proceedings of the*

Solid Freeform Fabrication Symposium, 2012.

[15] C. Kousiatza, N. Chatzidai, and D. Karalekas, "Temperature Mapping of 3D Printed Polymer Plates: Experimental and Numerical Study," *Sensors,* vol. 17, p. 456, 2017.

[16] X. Zhou, S.-J. Hsieh, and Y. Sun, "Experimental and numerical investigation of the thermal behaviour of polylactic acid during the fused deposition process," *Virtual and Physical Prototyping,* pp. 1-13, 2017.